



HAL
open science

Planar lossy filters for satellite transponders

Stéphane Bila, Ahmed Basti, Aurélien Perigaud, Serge Verdeyme, Laetitia Estagerie, Ludovic Carpentier, Hervé Leblond

► **To cite this version:**

Stéphane Bila, Ahmed Basti, Aurélien Perigaud, Serge Verdeyme, Laetitia Estagerie, et al.. Planar lossy filters for satellite transponders. *Advances in Planar Filters Design*, Institution of Engineering and Technology, pp.89-119, 2019, 10.1049/sbew535e_ch4 . hal-02377033

HAL Id: hal-02377033

<https://unilim.hal.science/hal-02377033>

Submitted on 16 Dec 2020

HAL is a multi-disciplinary open access archive for the deposit and dissemination of scientific research documents, whether they are published or not. The documents may come from teaching and research institutions in France or abroad, or from public or private research centers.

L'archive ouverte pluridisciplinaire **HAL**, est destinée au dépôt et à la diffusion de documents scientifiques de niveau recherche, publiés ou non, émanant des établissements d'enseignement et de recherche français ou étrangers, des laboratoires publics ou privés.

Chapter 4

Planar Lossy Filters for Satellite Transponders

Authors: Stéphane Bila, Ahmed Basti, Aurélien Périgaud, Serge Verdeyme, Laetitia Estagerie, Ludovic Carpentier, Hervé Leblond

4.1. Introduction

Microwave filters are key elements in many communication systems. Regarding the system and the position of the filter within the system, its design has to deal with particular electrical specifications and constraints that concern its weight and footprint. For instance, in satellite transponders, high quality factor (Q) filters based on cavities or dielectric resonators are required for output multiplexers, which have to cope with severe specifications in terms of insertion losses and power handling. For filters in the receiver part, the insertion loss and power handling performances are less critical, allowing the usage of more compact technologies, which make easier the integration with active circuits also.

For a receive filter, the challenge is to design a compact bandpass filter with a flat response in the passband and a sharp transition in the passband edges. The insertion loss is not crucial, since it does not affect the total noise factor as the filter is placed after the low-noise amplifier (LNA) and it can be compensated by the amplifier, leaving a room to the design of a lossy filter. Such a filter accepts additional losses, which can be distributed in the network in order to provide a flat transmission in the passband and a sharp selectivity.

This new class of microwave filters has been proposed recently in [1]-[6], and can be divided into two families mainly. Additional losses are introduced either in individual resonators, forming a network with non-uniform- Q resonators [3]-[4], or distributed through resistive cross-couplings [4]-[6].

In this literature, lossy filter prototypes are realized using different technologies and working frequencies making the comparison between different approaches difficult. In this chapter, the two approaches are compared considering the same specifications and the same technology. A classical filter is designed and fabricated first. Afterwards, lossy filters formed on the one hand by a transversal network with non-uniform Q resonators and, on the other hand, by an in-line network with resistive cross couplings are designed and fabricated for comparison. Finally, absorptive lossy filters are designed and fabricated. Such filters integrate the property of attenuating reflected wave that is often a requirement for protecting the receiver subsystem.

4.2. Impact of losses on filter performances

4.2.1. Relation between quality factor and insertion losses

The unloaded quality factor is related to the resonator technology (coaxial, dielectric, planar structure, superconductor ...). Generally, high Q resonators are physically larger and require the use of more expensive technology. For example, dielectric resonator filters can offer a very high quality factor [7], but their volume and cost is much higher than filters in microstrip technology [8]. It is shown in [9], that insertion losses (IL) are inversely proportional to the unloaded quality factor Q_u . For instance, insertion losses in the middle of the bandwidth of a Tchebychev-type bandpass filter can be estimated by:

$$IL = 8.686[N - 1.5] \frac{f_0}{\Delta_f Q_u} \quad (1)$$

Where N is the degree of the filter, f_0 its center frequency and Δ_f its passband.

Physically, this relationship can be explained by the fact that the group delay of the filter is inversely proportional to its bandwidth. Thus, for a given quality factor, the more the signal remains in the filter, the greater the losses are. In addition, the group delay of a filter always increases near the edges of the bandwidth. Thus, insertion losses near the edges of the bandwidth will be higher than the value in the middle of the bandwidth. Assuming a filter with a uniform distribution of the quality factor between resonators and a cutoff pulsation $\omega = 1 \text{ rad.s}^{-1}$, the increase in insertion losses can be estimated as [10]:

$$\Delta IL(\omega) \approx 8.686 \left(\frac{T_g(\omega)}{Q_u} \right) \quad (2)$$

Figure 4.1 shows the variation of insertion losses as a function of different Q values. One can observe a degradation of the flatness in the passband, which results in a rounding of passband edges. This variation, associated with less distinct transmission zeros, results in a degradation of the out-of-band rejections.

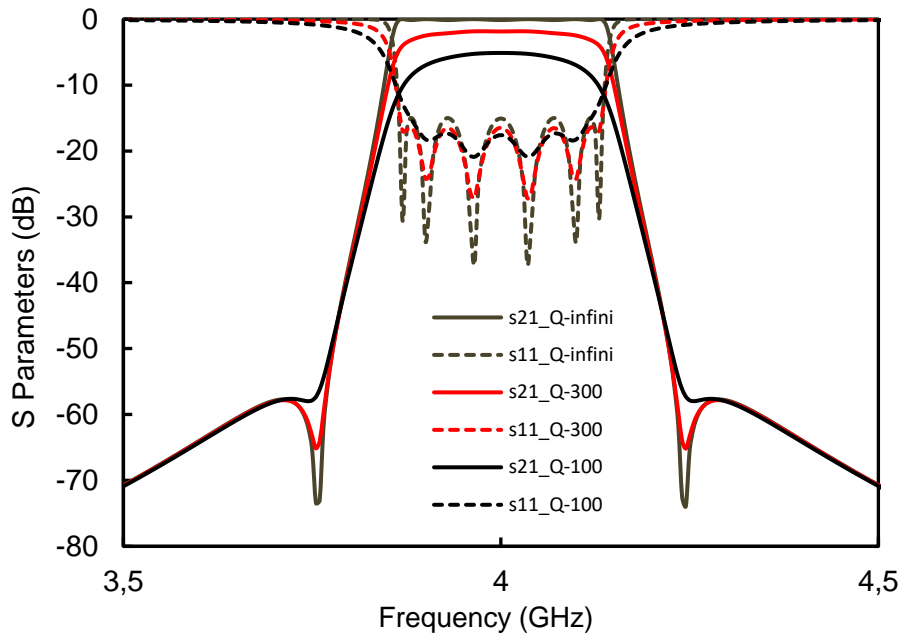


Figure 4.1. Filter responses for different values of the unloaded quality factor

Figure 4.2 shows the displacement of the poles of the transfer function in the complex plane in the ideal case without losses (infinite Q) and the real case with losses (finite Q). Taking into account losses in the transfer function causes the poles to shift to the left in the complex plane. This shift is inversely proportional to the quality factor of the resonators:

$$\alpha = \frac{Q_p - Q_0}{Q_p} \quad (3)$$

where Q_0 is the quality factor of the initial filtering function and Q_p is that of the modified function.

If all the resonators have the same finite quality factor, it is therefore possible to evaluate the offset α and compensate it upstream to maintain the same transfer function, excepted a fix amount losses.

This predistortion technique has been the subject of several studies [11] - [14].

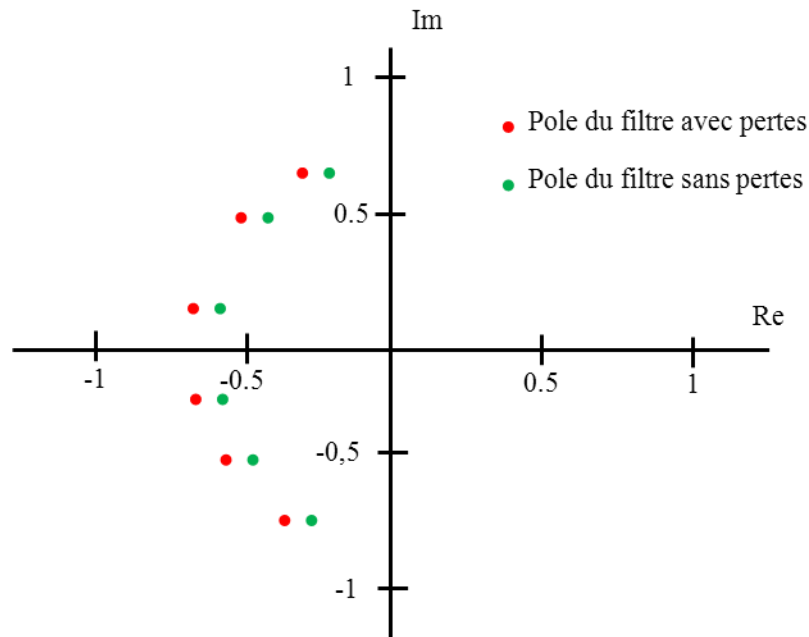


Figure 4.2. Typical displacement of the poles in the complex plane, considering finite and infinite quality factors (example of a 6 pole transfer function)

4.2.2. Compensation by predistortion

The predistortion technique, which was developed in 1940 [13], is a method of total or partial compensation. The principle is to shift the poles (p) of the transfer function to the right of the complex plane:

$$p \rightarrow p - \alpha \quad (4)$$

Thus, the transfer function of the filter in presence of losses corresponds to a conventional lossless transfer function, with a constant additional attenuation, whatever the frequency.

There are some disadvantages associated with the predistortion technique, which suffers from poor bandwidth adaptation. Indeed, the polynomial reflection function is evaluated by applying the relation of conservativity, and the displacement of poles and zeros of reflection destroys the matching condition. It should be noted that this approach leads to several solutions [13] for the realization of the filter since several choices are possible to determine the reflection zeros.

In order to limit the previous disadvantages, an adaptive or partial predistortion can be applied in order to compensate the rounding of the bandwidth edges while keeping a correct matching. Details of these techniques are presented respectively in [12] and [14].

Relatively high return loss levels limit the use of these filters to systems or subsystems where the power level is low. In the payload of a satellite, these filters are used for input multiplexers, placing a circulator that directs the reflected signal to a suitable load. Since the input signal of the input multiplexer is relatively weak, the power dissipated by the load remains low. The subsystem introduces more losses but makes it possible to limit the variation in amplitude in the bandwidth with a smaller device.

4.2.3. Synthesis of lossy filters

The synthesis of lossy filters is intended to achieve a filter having an improved flatness in the bandwidth, playing on the distribution of losses. Thus, compared to a filter resulting from a conventional synthesis, this type of filter will have for a number of resonators and a given maximum quality factor, a higher relative loss level but a flatness equivalent to a much higher quality factor. In comparison with the predistortion technique, this approach degrades the level of adaptation much less. Figure 4.3 shows the expected filter response for different Q values in the case of lossy synthesis. One can see a decline of insertion loss, but still a very flat and very selective response. This result is obtained by using resonators with different quality factors and / or introducing lossy couplings. In the following paragraphs, different approaches proposed in the literature for lossy filter synthesis are presented.

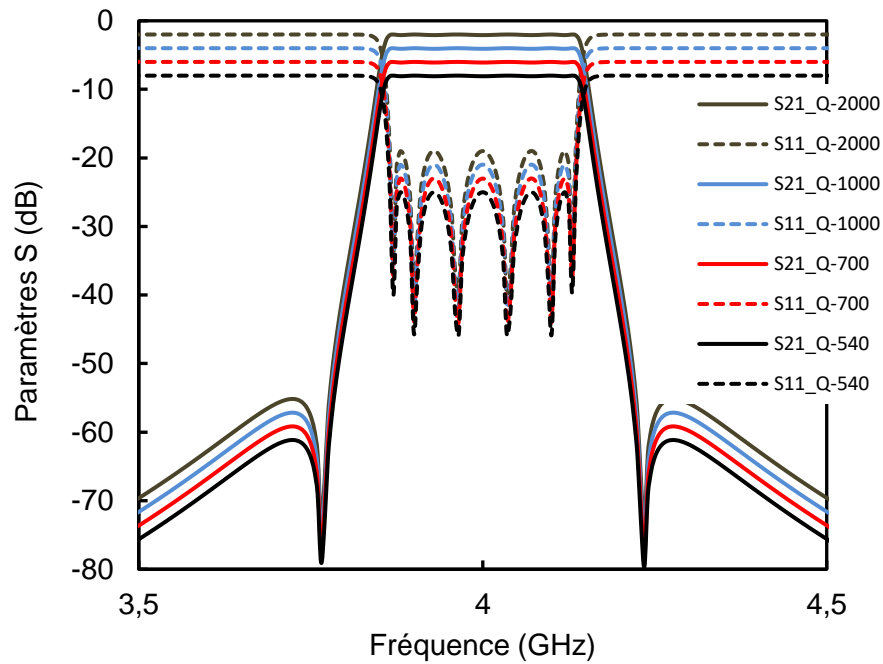


Figure 4.3. Lossy filter response for different Q values

1) Lossy resonators and resistive cross couplings for optimizing transfer function

The first approach, proposed in [15], consists in multiplying the polynomial lossless transfer function by a constant attenuation factor $K < 1$. This transfer function includes finite losses; consequently, the condition of unit conservativity connecting scattering parameters S_{21} and S_{11} does not apply. Thus, it is difficult to understand how to form the reflection function and then the input impedance, in order to synthesize the network exactly. This problem is solved using a new pre-distortion technique, which is applicable only in the case of a symmetric quadripole, where an approximation can be made to compute S parameters, based on the theory of odd and even modes. The network comprises coupled resonators with different Q factors at its input and output.

An improvement of this technique is presented in [16]. The technique consists in distributing the losses created by attenuation factor K . Losses are distributed through the network by adding a finite pole-zero pair to the loss transfer function. The additional pole corresponds to the addition of a resonator within the network, while the additional zero creates a parallel signal transmission path. These additional elements make possible to improve electrical performance, including flatness in the passband, matching and selectivity. The parallel path is made by simply placing a resistor between two non-adjacent resonators of the network to create a non-resonant resistive coupling.

2) Resistive couplings and non-resonating nodes for attenuating transfer and reflection functions

The previous approach is extended in [4] and [5] considering different attenuation factors $K_{ij} < 1$ for transfer and reflection functions. In this general case, several methods for direct synthesis of the lossy coupling matrix have been developed in the literature [4]-[6], [17] [18].

A special case is to consider a constant attenuation ($K_{11} = K_{21} = K_{22} = K < 1$). From a network point of view, this particular case is equivalent to placing two identical attenuators at the input and output ports of a lossless filter. In the general case, the synthesis technique makes possible to have filtering functions with different attenuation levels for the input and output reflections [4].

It is then generally preferable to distribute the losses in the network using resistive couplings and non-resonant nodes [5] to simplify the manufacturing process. The distribution of losses within the network is achieved by applying a series of hyperbolic rotation on the complex coupling matrix.

3) Filter networks with heterogeneous Q resonators

Initially, the preferred way to implement lossy filters was to introduce resistive couplings. In some cases, the introduction of resonators with different quality factors can further optimize performance. On the other hand, several authors proposed the implementation of lossy filters based solely on heterogeneous quality factor resonators.

Ref. [19] shows that the flatness of the filter with resonators having non-uniform quality factors can be optimized by placing the

more dissipative elements at the ends of the network. Apart from an optimization of quality factors and couplings, the generalization of this approach has not been made.

Arranging the lossy filter into a transversal network allows optimizing the flatness in the bandwidth more easily, by controlling the distribution of losses through the parallel paths. In this case, each resonator or each path can be optimized to find the desired performance. A theoretical approach is presented in [3] to explain the influence of losses in each path of the transversal network.

4) *Lossy redundant structures*

In order to be relatively comprehensive in our description, we have to report on a different approach developed as in [20]. In this approach, the circuit is split into two subnetworks, one symmetrical and the other antisymmetrical, and each of these subnets is redundantly duplicated.

A compromise between redundancy (thus circuit size) and degrees of freedom in the design of the filter is necessary. These degrees of freedom can be exploited to play with the return loss and the selectivity or reduce the quality factors of resonators.

The technique consists in determining the even and odd sub-networks. This step is generally followed by a simplification in order to reduce the network toward N resonators (non-redundant network).

4.3. Reference design: hairpin microstrip filter

The objective of this work is to design a compact microstrip filter centered at 3.8 GHz with an 800-MHz bandwidth, considering the specifications detailed in Table 4.1. The initial design is achieved by a hairpin microstrip filter. The resonators are fabricated on an alumina substrate having a height of 0.254 mm. The substrate permittivity is $\epsilon_r = 9.9$ and its loss tangent is $\tan \delta = 0.0002$. The metallization is 5 μm thick. Using this technology, the unloaded quality factor of each hairpin resonator is around 95. In order to fulfill the previous requirements, a six-pole Chebyshev transfer function is synthesized [19]. The synthesized response is given in Figure 4.4. The response fulfills the specifications, except for the flatness, which attains 1 dB.

Table 4.1 - Specifications for this work. Reprinted with permission from ref. [1]; copyright 2014 IEEE.

Parameter	Value	Unit
Center frequency (f_0)	3800	MHz
Bandwidth	800	MHZ
Insertion loss (IL)	< 5	dB
Flatness (IL variation)	< 0.7	dB
Return loss (RL)	> 18	dB
Attenuation at $f_0 \pm 1000$ MHz	35	dBc
Attenuation at $f_0 \pm 2000$ MHz	20	dBc

The filter can be structured either as an in-line network or as a transversal network, as shown in Figs. 5 and 6. One can note that the transversal network is a transversal pair network, since this particular topology is a practical form for implementing lossy filters. The corresponding coupling matrices are given together with the two coupling networks. Diagonal terms ($j0.05$) in the coupling matrices are placed here for modeling the finite Q value of resonators.

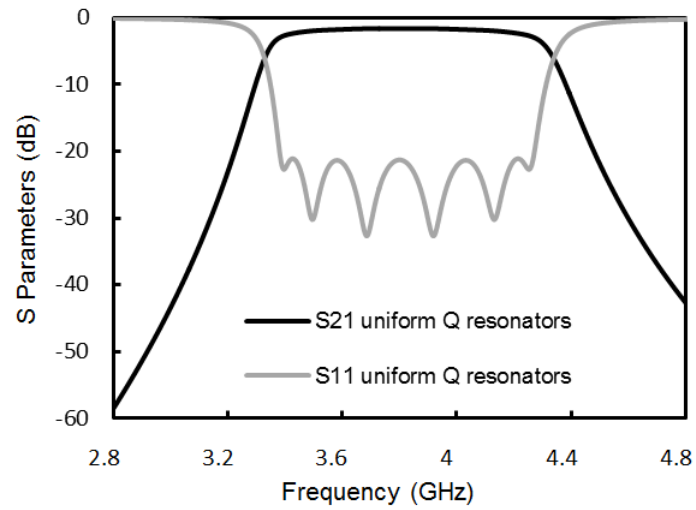
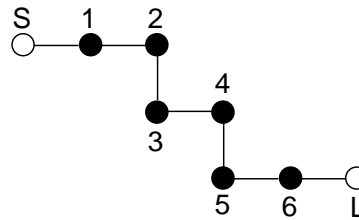


Figure 4.4 – Synthesized (Chebyshev) response for the classical hairpin filter (reference design with uniform-Q resonators). Reprinted with permission from ref. [1]; copyright 2014 IEEE.

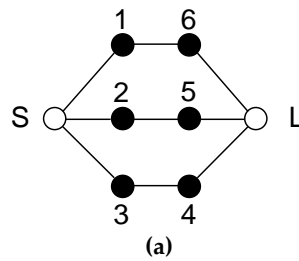


(a)

	S	1	2	3	4	5	6	L
S	0	1.002	0	0	0	0	0	0
1	1.002	$j0.05$	0.843	0	0	0	0	0
2	0	0.843	$j0.05$	0.611	0	0	0	0
3	0	0	0.611	$j0.05$	0.583	0	0	0
4	0	0	0	0.583	$j0.05$	0.611	0	0
5	0	0	0	0	0.611	$j0.05$	0.843	0
6	0	0	0	0	0	0.843	$j0.05$	1.002
L	0	0	0	0	0	0	1.002	0

(b)

Figure 4.5 - Coupling diagram (a) and coupling matrix (b) for realizing the initial filter as an in-line network with uniform-Q resonators ($Q=95$). Reprinted with permission from ref. [1]; copyright 2014 IEEE.



(b)

	S	1	2	3	4	5	6	L
S	0	0.638	0.629	0.447	0	0	0	0
1	0.638	$j0.05$	0	0	0	0	0.356	0
2	0.629	0	$j0.05$	0	0	-0.971	0	0
3	0.447	0	0	$j0.05$	1.199	0	0	0
4	0	0	0	1.199	$j0.05$	0	0	0.447
5	0	0	-0.971	0	0	$j0.05$	0	0.629
6	0	0.356	0	0	0	0	$j0.05$	0.638
L	0	0	0	0	0.447	0.629	0.638	0

Figure 4.6 - Coupling diagram (a) and coupling matrix (b) for realizing the initial filter as a transversal network with uniform- Q resonators ($Q=95$). Reprinted with permission from ref. [1]; copyright 2014 IEEE.

The reference filter is implemented as an in-line network using hairpin resonators as shown in Figure 4.7. The structure has a surface of 210 mm². The simulations have been performed using *Momentum*[™] included in Agilent *Advanced Design System*[™] (ADS) and dimensions have been optimized by parameter extraction [20]. A prototype has been fabricated and measured. The comparison between measured and simulated responses is presented in Figure 4.8. A slight reduction in the bandwidth is observed compared to EM simulations. The return loss in the bandwidth is still better than 20 dB and the insertion loss is comparable to the simulated one, around 1.9 dB. The measured flatness is 1.2 dB, *i.e.* slightly degraded compared to the theory.



Figure 4.7 – Layout of the classical Chebyshev filter implemented as aligned hairpin coupled resonators. Reprinted with permission from ref. [1]; copyright 2014 IEEE.

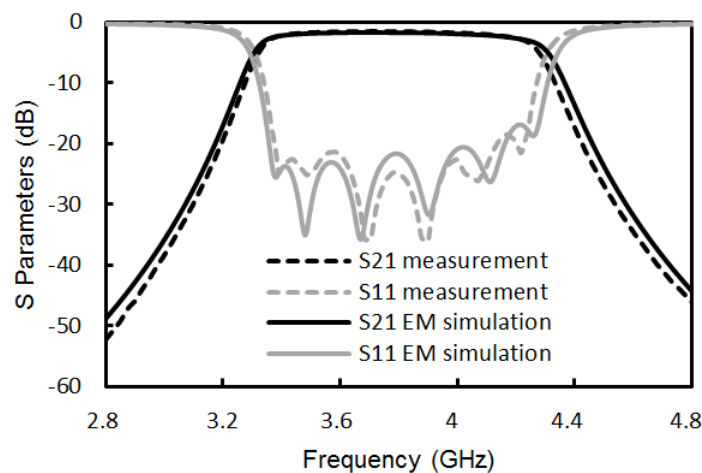


Figure 4.8 - Classical Chebyshev filter : measurements and EM simulation. Reprinted with permission from ref. [1]; copyright 2014 IEEE.

In order to explain the difference between measurements and full wave simulations, a sensitivity analysis has been performed considering typical manufacturing tolerances. An 8- μm tolerance for transmission line dimensions and a 1%-variation in the permittivity value have been considered for the Monte-Carlo analysis performed with Agilent ADS and presented in Figure 4.9. The permittivity variation mainly affects the frequency, while geometrical variations also affect the return loss. Excluding flatness constraints, more than 70% of realizations meet the specifications.

The objective of this work is now to improve the flatness by designing lossy filters, considering margins available on the insertion losses. Several approaches are compared. The electrical performances of this conventional filter serve as reference for the next designs.

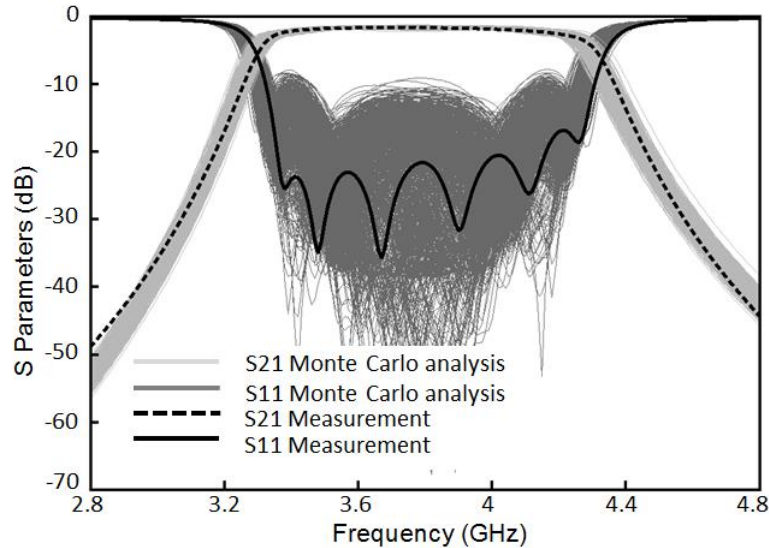


Figure 4.9 – Classical Chebyshev filter : Monte-Carlo analysis considering typical manufacturing tolerances (8 μm for transmission line dimensions and 1% for relative permittivity). Reprinted with permission from ref. [1]; copyright 2014 IEEE.

4.4. Design of lossy filters for improved flatness

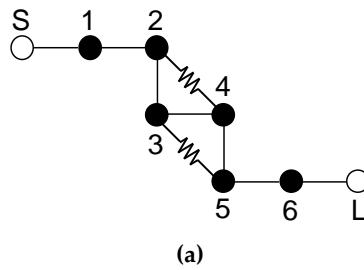
The principle of lossy filters consists to add and to distribute losses into the coupled-resonator network for retrieving a lossless-like transfer function, *i.e.* having the same flatness and the same selectivity, at a sacrifice on the absolute level of losses. Two ways are possible for realizing a lossy filter. The first way consists in introducing losses in the network through resistive cross-couplings [18] and the second in introducing additional losses directly within some resonators [3]. These two approaches may be mixed also [16]. In this work, lossy filters are designed, on one hand as in-line networks with resistive cross-couplings and on the other hand as transversal networks with heterogeneous- Q resonators.

4.4.1. In-line network with resistive cross couplings

The introduction of resistive cross-couplings (RCCs) in the network allows adjusting the flatness in the passband [22], [17]. The number of RCCs in the network is an important parameter, which impacts the performance of the filter directly, in particular its insertion loss and flatness.

For comparison, two lossy filters have been synthesized, with 2 and 4 resistive cross-couplings respectively, using the approach and software developed in [21] and [22] respectively. The coupling diagrams and coupling matrices can be found in Figs. 10 and 11. The lossy filter responses are compared together with the classical filter response in Figure 4.12. One can observe a slight reduction in the selectivity for the lossy filters.

The flatness is around 0.4 dB for the structure with 2 RCCs and 0.3 dB for the structure with 4 RCCs. At the same time, the insertion loss is found to be 3.4 dB for the first filter (2 RCCs) and 4.2 dB for the second one (4 RCCs). The RCCs are implemented using engraved Ta2N resistors ($R_{\square} = 50 \Omega.\text{sq}$) placed between quarter-wave transmission lines, as shown in Figure 4.13.

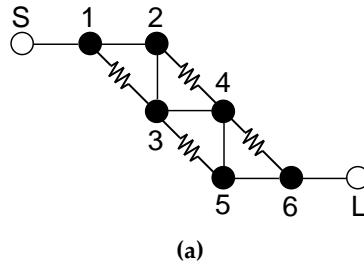


(a)

	S	1	2	3	4	5	6	L
S	0	1.304	0	0	0	0	0	0
1	1.304	$j0.059$	1.191	0	0	0	0	0
2	0	1.191	$j0.091$	0.696	$j0.031$	0	0	0
3	0	0	0.696	$j0.091$	0.679	$j0.031$	0	0
4	0	0	$j0.031$	0.679	$j0.091$	0.696	0	0
5	0	0	0	$j0.031$	0.696	$j0.091$	1.191	0
6	0	0	0	0	0	1.191	$j0.059$	1.304
L	0	0	0	0	0	0	1.304	0

(b)

Figure 4.10 – Coupling diagram (a) and coupling matrix (b) of the in-line network with 2 RCCs. Reprinted with permission from ref. [1]; copyright 2014 IEEE.



(a)

	S	1	2	3	4	5	6	L
S	0	1.304	0	0	0	0	0	0
1	1.304	$j0.064$	1.168	$j0.004$	0	0	0	0
2	0	1.168	$j0.115$	0.713	$j0.055$	0	0	0
3	0	$j0.004$	0.713	$j0.119$	0.675	$j0.055$	0	0
4	0	0	$j0.055$	0.675	$j0.119$	0.713	$j0.004$	0
5	0	0	0	$j0.055$	0.713	$j0.115$	1.168	0
6	0	0	0	0	$j0.004$	1.168	$j0.064$	1.304
L	0	0	0	0	0	0	1.304	0

(b)

Figure 4.11 – Coupling diagram (a) and coupling matrix (b) of the in-line network with 4 RCCs. Reprinted with permission from ref. [1]; copyright 2014 IEEE.

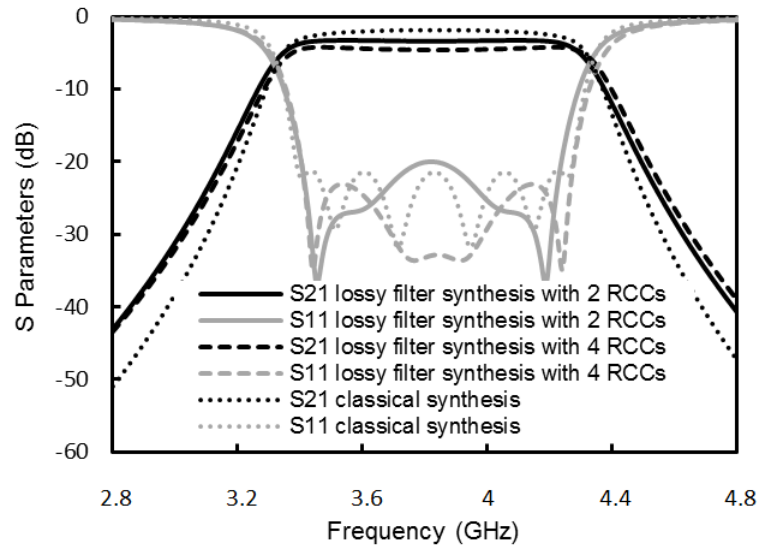
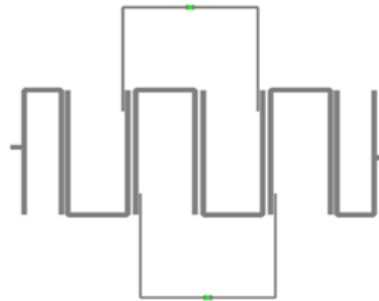
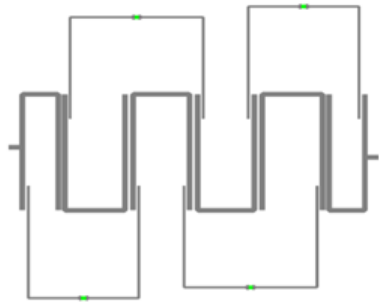


Figure 4.12. – Synthesized responses for the lossy filters with 2 and 4 RCCs. Reprinted with permission from ref. [1]; copyright 2014 IEEE.



(a)



(b)

Figure 4.13 – Layout of lossy filters implemented as in-line coupled hairpin resonators with (a) two RCCs and (b) four RCCs. Reprinted with permission from ref. [1]; copyright 2014 IEEE.

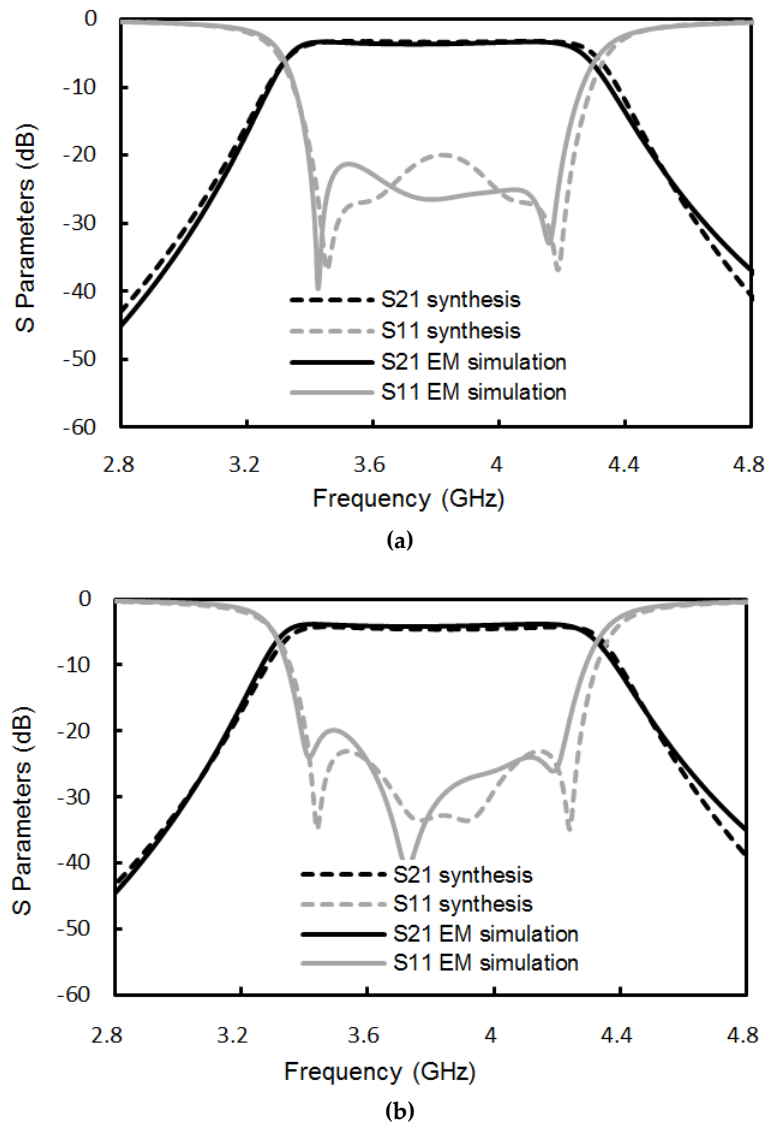
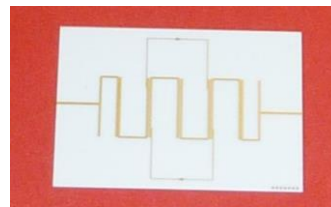
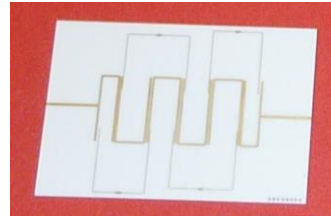


Figure 4.14 – Simulated response of the lossy filters with (a) two RCCs and (b) four RCCs. Reprinted with permission from ref. [1]; copyright 2014 IEEE.

The filters were designed and optimized by parameter extraction using *Momentum*[™] for full wave simulations. Figure 4.14 shows the simulated scattering parameters compared to theoretical ones for both lossy filters. The lossy filter with two RCCs presents a flatness of 0.4 dB, with a maximum insertion loss of 3.1 dB. The lossy filter with four RCCs presents a flatness of 0.3 dB, and a maximum insertion loss of 4.2 dB. The filters were fabricated using the previous substrate. A photography is displayed in Figure 4.15. The lossy filter with 2 RCCs has a size of 290 mm² and the lossy filter with 4 RCCs a size of 300 mm². Measurements are presented in Figure 4.16. The measured performances remain comparable to the simulated ones for the two fabricated filters except a slight reduction in the bandwidth and a slight degradation of the flatness (+0.1 dB).

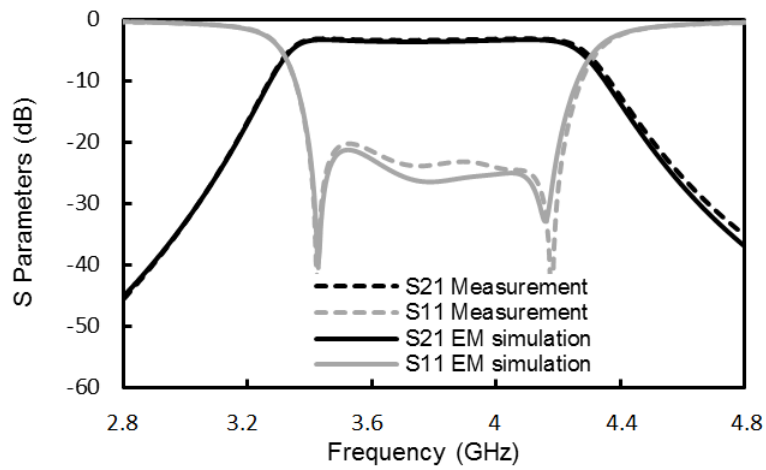


(a)

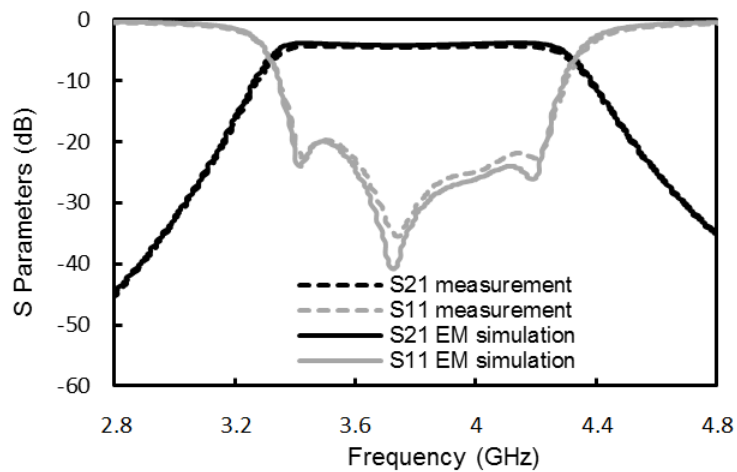


(b)

Figure 4.15 – Fabricated lossy filters with (a) two RCCs and (b) four RCCs Reprinted with permission from ref. [1]; copyright 2014 IEEE.



(a)



(b)

Figure 4.16 – Lossy filters with (a) two RCCs and (b) four RCCs : measurements and EM simulations. Reprinted with permission from ref. [1]; copyright 2014 IEEE.

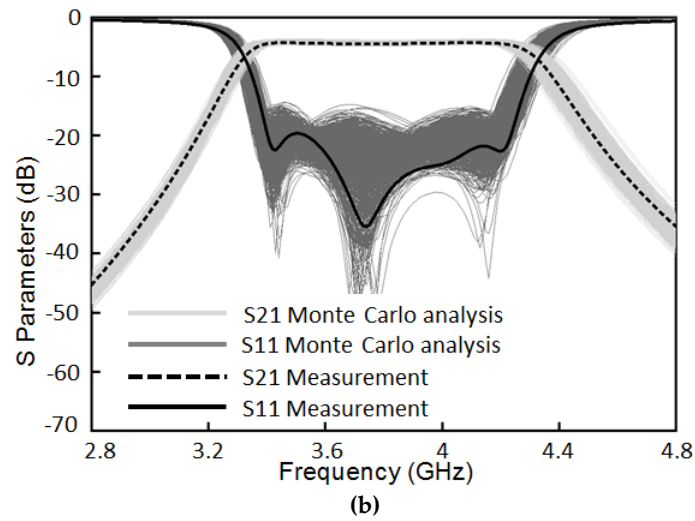
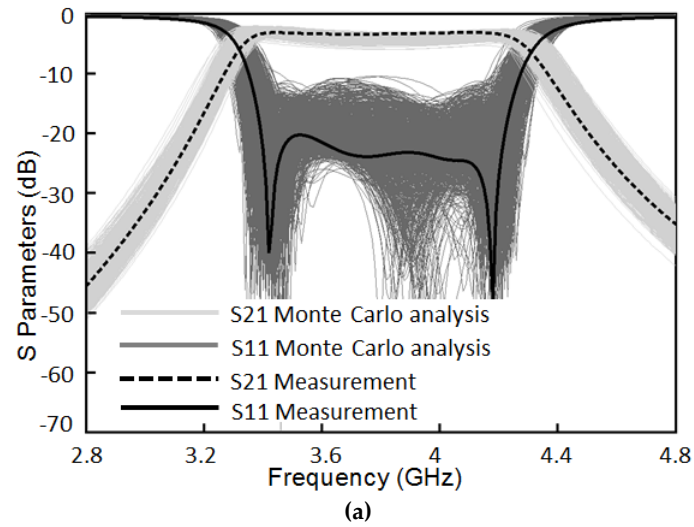


Figure 4.17 – Lossy filters with (a) two RCCs and (b) four RCCs: Monte-Carlo analysis considering typical manufacturing tolerances (8 μm for transmission line dimensions, 1% for relative permittivity, and 2% for engraved resistors). Reprinted with permission from ref. [1]; copyright 2014 IEEE.

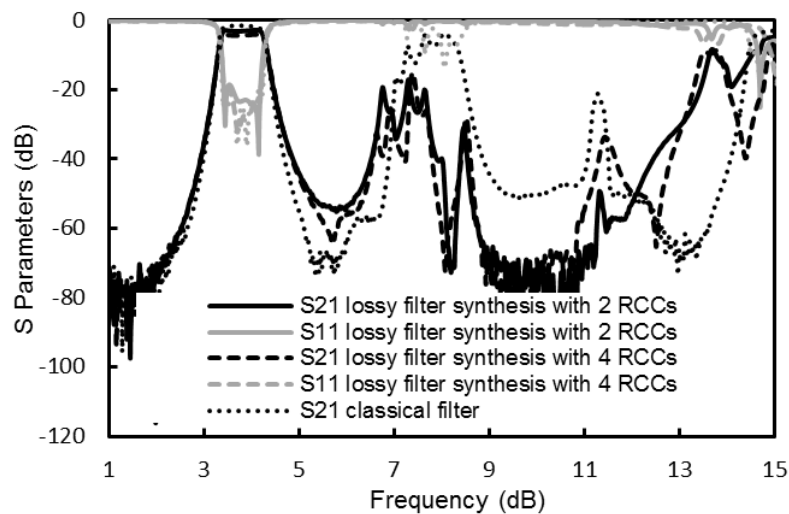


Figure 4.18 – Measured out-of-band performances for lossy filters with resistive cross-couplings. Reprinted with permission from ref. [1]; copyright 2014 IEEE.

A Monte-Carlo analysis has been performed considering the same manufacturing tolerances. A 2% tolerance is also considered for engraved resistors. Figure 4.17 compares the measurements together with the Monte-Carlo analysis. About 65% of realizations met the specifications for the filter with 2 RCCs, and 60% considering the filter with 4 RCCs.

Performances at higher frequency are displayed in Figure 4.18. One can observe that lossy filters provide better attenuation of the second harmonic.

The lossy filter with two RCCs satisfies all the specifications. Adding two additional resistive cross-couplings provides a very small improvement in terms of flatness, while the degradation of insertion loss becomes significant. The equivalent quality factor (Q) of the lossy filter with two RCCs is about 300, *i.e.* three times higher compared to the real one.

4.4.2. Transversal network with non-uniform Q resonators

In the case of a transversal network, the signal follows multiple paths. Each path contributes in the filter response almost independently. Using a transversal pair network, the path comprising the stronger coupled resonators mainly contributes to insertion loss in the passband edges. For these resonators, the higher the Q is, the higher the selectivity is. Moreover, the insertion loss is also maximized in the passband edges; consequently these resonators need to be high- Q . Other paths, *i.e.* with weakly coupled resonators, contribute to insertion loss in the middle of the passband. Consequently, the quality factor of such resonators can be degraded for increasing the insertion loss in the middle of the passband, reducing by this way the insertion loss variation in the bandpass filter response.

The transversal pair network presented in Figure 4.19 can be synthesized as a lossy filter network by optimizing a coupling matrix obtained from a general Chebyshev filtering function, as introduced in [19]. Initially, a coupling matrix with uniform Q resonators is considered. The synthesis consists in optimizing the couplings and the quality factors of each pair for achieving the desired performances. It is clear that the quality factors can only be degraded in this case.

In order to fit with the specifications in Table 4.1, the coupling matrix synthesized from the Chebyshev filtering function (Figure 4.6) is optimized considering now non-uniform Q resonators using a lumped element equivalent circuit defined with Agilent ADSTM. The optimized coupling matrix is given in Figure 4.20. The imaginary parts of diagonal terms in the coupling matrix reflect the quality factors of individual resonators. One can see that Q factors are degraded from 95 ($r_i=0.05$) respectively to 57 ($r_i=0.08$) and 35 ($r_i=0.13$) in the two other paths.

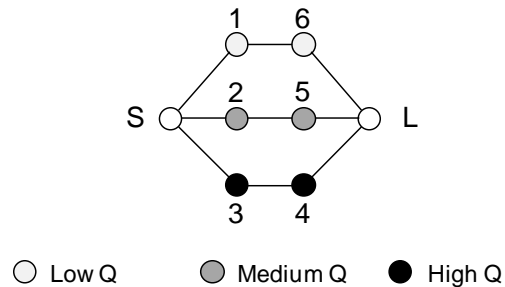


Figure 4.19. – Six-pole transversal filter network with non-uniform Q resonators. Reprinted with permission from ref. [1]; copyright 2014 IEEE.

	S	1	2	3	4	5	6	L
S	0	0.653	0.645	0.462	0	0	0	0
1	0.653	$j0.13$	0	0	0	0	0.374	0
2	0.645	0	$j0.08$	0	0	-1.026	0	0
3	0.462	0	0	$j0.05$	1.249	0	0	0
4	0	0	0	1.249	$j0.05$	0	0	0.462
5	0	0	-1.026	0	0	$j0.08$	0	0.645
6	0	0.374	0	0	0	0	$j0.13$	0.653
L	0	0	0	0	0.462	0.645	0.653	0

Figure 4.20 - Coupling matrix of transversal network with non-uniform Q resonators. Reprinted with permission from ref. [1]; copyright 2014 IEEE.

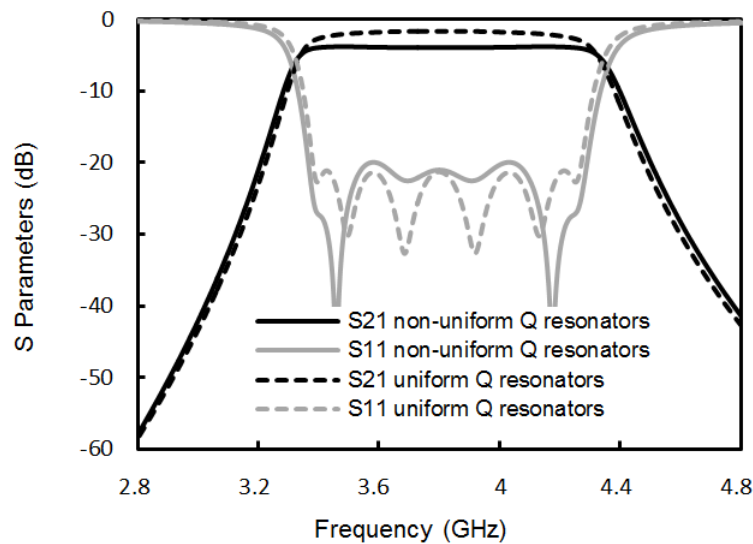


Figure 4.21 - Synthesized response of the transversal network with non-uniform Q resonators. Reprinted with permission from ref. [1]; copyright 2014 IEEE.

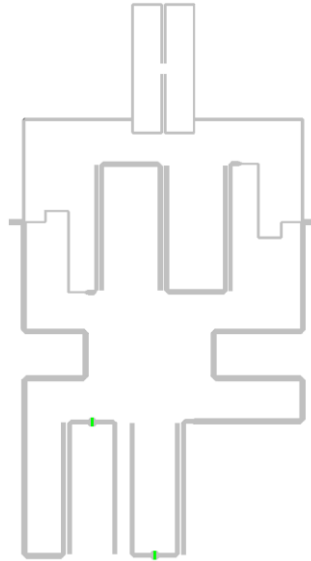


Figure 4.22 - Layout of the transversal filter with non-uniform Q resonators. Reprinted with permission from ref. [1]; copyright 2014 IEEE.

The initial and optimized responses are compared in Figure 4.21. One can observe that the transversal network with non-uniform Q has improved performances in terms of flatness while maintaining a similar selectivity and return loss level. The insertion loss variation reaches now 0.1 dB in the passband (compared to 1 dB for the transversal network with uniform Q resonators) and the minimum insertion loss is around 3.3 dB (+ 1.7 dB compared to the transversal network with uniform Q resonators).

The filter is designed with *Momentum*TM using microstrip hairpin resonators. With 240- μm -wide lines, the achieved Q factor is equal to 95. By reducing the width at 70 μm , the Q factor is diminished to 57. In order to achieve a lower Q factor ($Q=35$), engraved resistors are introduced in the resonators. Figure 4.22 shows the layout of the six-pole transversal filter with non-uniform Q resonators. Its size covers 480 mm² and the scattering parameters obtained from EM simulations are shown in Figure 4.23.

The filter has been fabricated (Figure 4.24) and characterized. A good agreement is found between measurements and EM simulations as shown in Figure 4.25. Only a slight reduction in the bandwidth is observed. The fabricated filter presents an insertion loss variation of 0.4 dB, the minimum insertion loss is about 2.2 dB and the return loss is better than 18 dB.

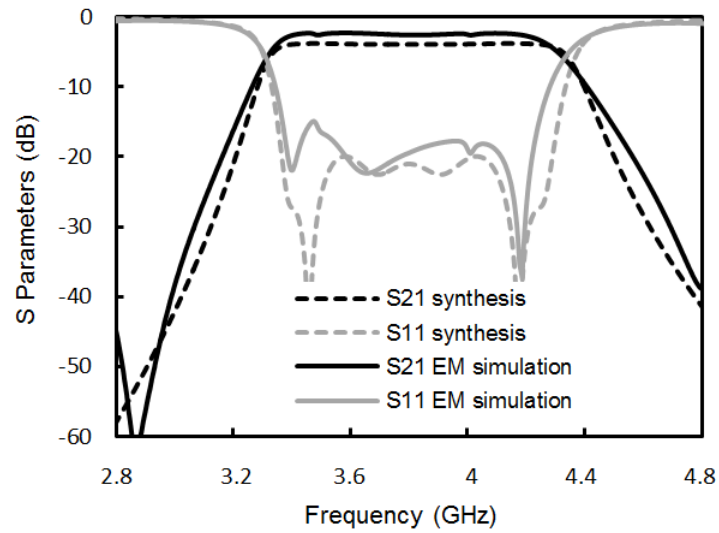


Figure 4.23 - Simulated response of the transversal filter with non-uniform Q resonators. Reprinted with permission from ref. [1]; copyright 2014 IEEE.

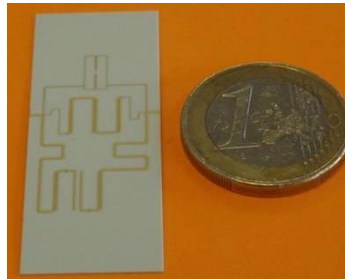
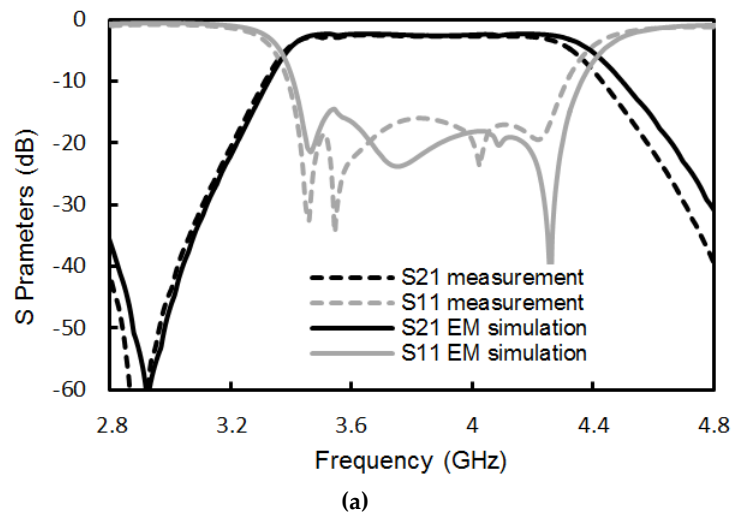


Figure 4.24 - Fabricated transversal filter with non-uniform Q resonators Reprinted with permission from ref. [1]; copyright 2014 IEEE.



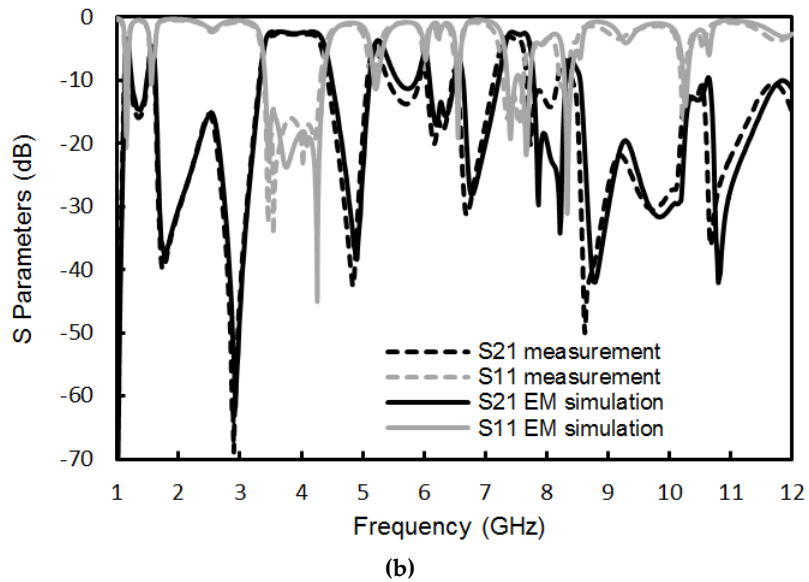


Figure 4.25 - Measurements of the transversal filter with non-uniform Q resonators: (a) around the passband and (b) in a broad band. Reprinted with permission from ref. [1]; copyright 2014 IEEE.

The sensitivity analysis presented in Figure 4.26 has been performed considering the previous tolerances. With this transversal design, only 37% of the realizations met the specifications. Moreover, evaluating the out-of-band performance, spurious transmissions are found close to the passband, violating the specifications in terms of rejection in the stopband. For this reason, the lossy filter with 2 RCCs is preferred for our application. However, the spurious transmission could be attenuated by introducing lowpass cells in the structure.

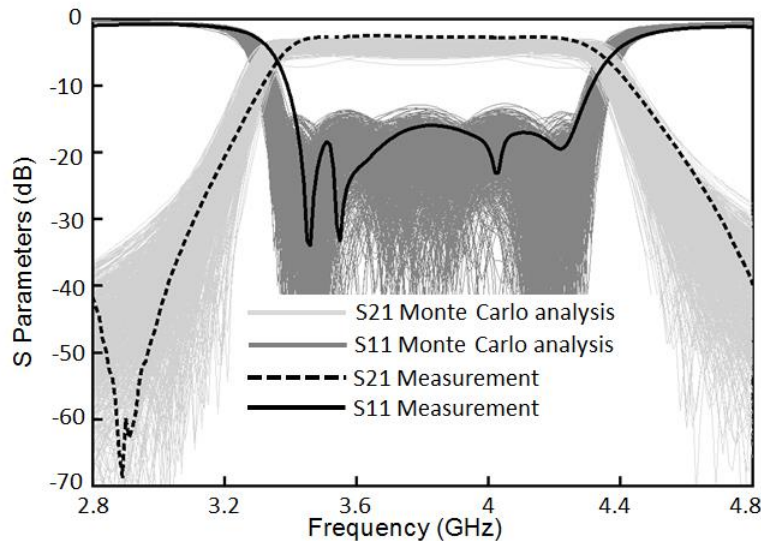


Figure 4.26 – Transversal lossy filter: Monte-Carlo analysis considering typical manufacturing tolerances ($8 \mu\text{m}$ for transmission line dimensions, 1% for relative permittivity, and 2% for engraved resistors). Reprinted with permission from ref. [1]; copyright 2014 IEEE.

4.5. Design of absorptive lossy filters for attenuation of reflected waves

A frequent need for the design of receivers is to attenuate reflected waves in the stopband in order to protect circuits placed before. The protection is generally achieved by introducing attenuators before the filter, which affect both the reflected and transmitted signals. Using lossy filters, the transmitted signal is already attenuated in order to improve the flatness. Attenuation of the reflected signal is then achieved by modifying slightly the architecture, without additional insertion loss in the passband.

Following the procedure detailed in [4], [16], [22], the attenuation is distributed together with the losses among the network, using

resistive couplings and non-resonating nodes (NRN). The previous in-line network has been modified as presented in Figure 4.27, in order to design two lossy filters with symmetric and asymmetric levels of attenuation.

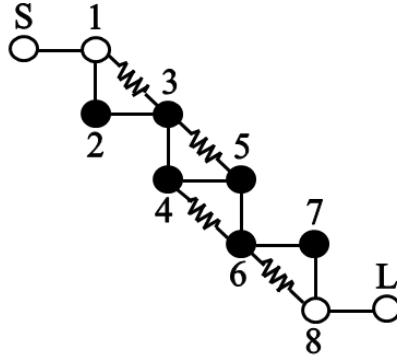


Figure 4.27. Coupling network for absorptive lossy filters (symmetric and asymmetric configurations). Reprinted with permission from ref. [1]; copyright 2014 IEEE.

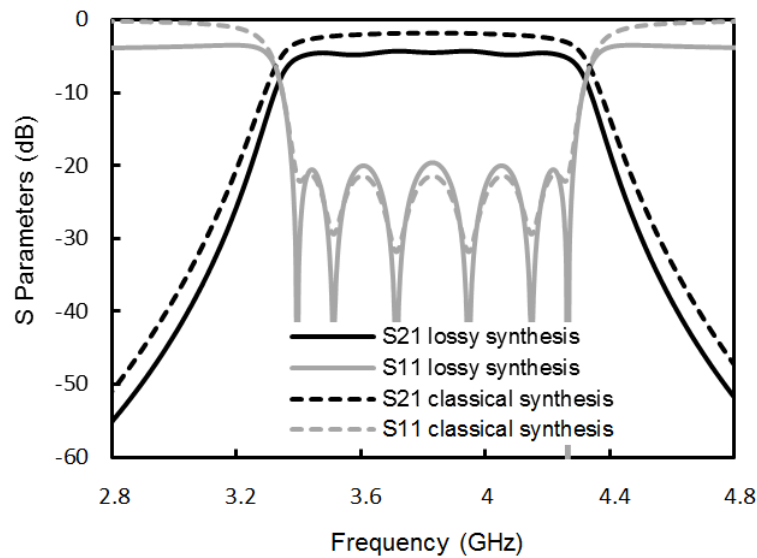


Figure 4.28 - Synthesized response of the symmetric absorptive lossy network. Reprinted with permission from ref. [1]; copyright 2014 IEEE.

4.5.1. Symmetric absorptive lossy filter

In this configuration, both the transmission and reflection functions will be attenuated with the same factor ($K = 0.63$). Figure 4.28 shows the ideal response of this filter, and the coupling matrix synthesized following the procedure detailed in [21] is given in Figure 4.29. Again, the filter is implemented using microstrip hairpin resonators as shown in Figure 4.30. The filter is dimensioned by parameter extraction from full wave simulations with *Momentum*TM. The simulated scattering parameters are presented in Figure 4.31. As expected, the attenuation in the stopband is around 4 dB ($K = 0.63$). The insertion loss is slightly higher (4.3 dB) and the insertion loss variation attains 0.6 dB. The filter was fabricated using the same substrate (Figure 4.32). Measurements in Figure 4.33 are found in good accordance with the simulation, except a slight reduction in the bandwidth and a slight degradation of the flatness (+0.05 dB).

	S	1	2	3	4	5	6	7	8	L
S	0	0.3662	0	0	0	0	0	0	0	0
1	0.3662	j0.0315	-0.3173	j0.0051	0	0	0	0	0	0
2	0	-0.3173	j0.0529	0.8326	0	0	0	0	0	0
3	0	j0.0051	0.8326	j0.0753	0.5969	j0.0175	0	0	0	0
4	0	0	0	0.5969	j0.0977	0.5384	j0.0449	0	0	0
5	0	0	0	j0.0175	0.5384	j0.0701	0.5969	0	0	0
6	0	0	0	0	j0.0449	0.5969	j0.2330	0.8326	j0.1352	0
7	0	0	0	0	0	0	0.8326	j0.0527	-0.3173	0
8	0	0	0	0	0	0	j0.1352	-0.3173	j0.0670	0.3662
L	0	0	0	0	0	0	0	0	0.3662	0

Figure 4.29 - Coupling matrix of the symmetric absorptive lossy network. Reprinted with permission from ref. [1]; copyright 2014 IEEE.

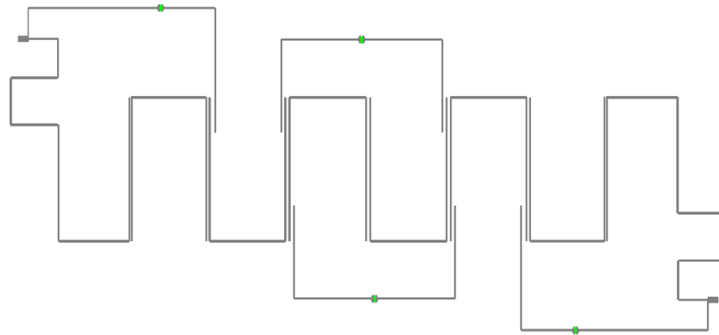


Figure 4.30 - Layout of the symmetric absorptive lossy filter. Reprinted with permission from ref. [1]; copyright 2014 IEEE.

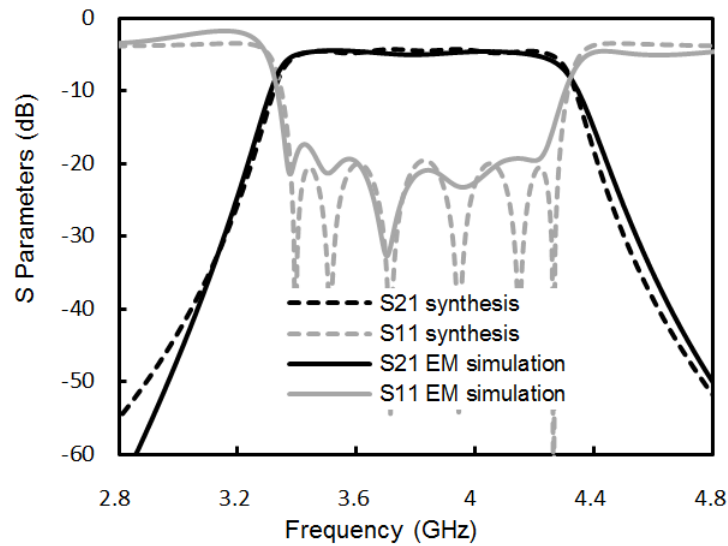


Figure 4.31 - Simulated response of the symmetric absorptive lossy filter. Reprinted with permission from ref. [1]; copyright 2014 IEEE.

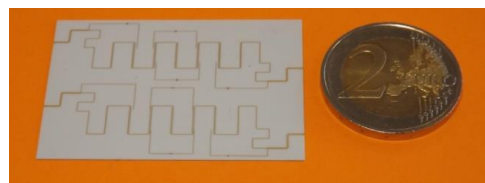


Figure 4.32 - Fabricated absorptive lossy filters (symmetric and asymmetric attenuations). Reprinted with permission from ref. [1]; copyright 2014 IEEE.

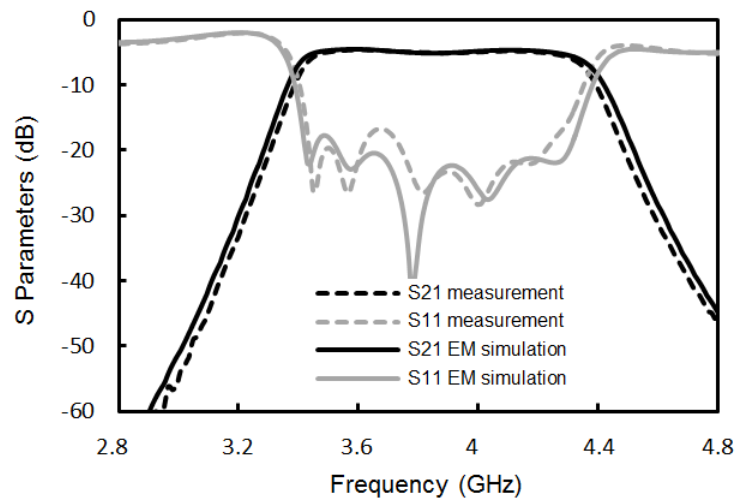


Figure 4.33 - Measured response of the symmetric absorptive lossy filter. Reprinted with permission from ref. [1]; copyright 2014 IEEE.

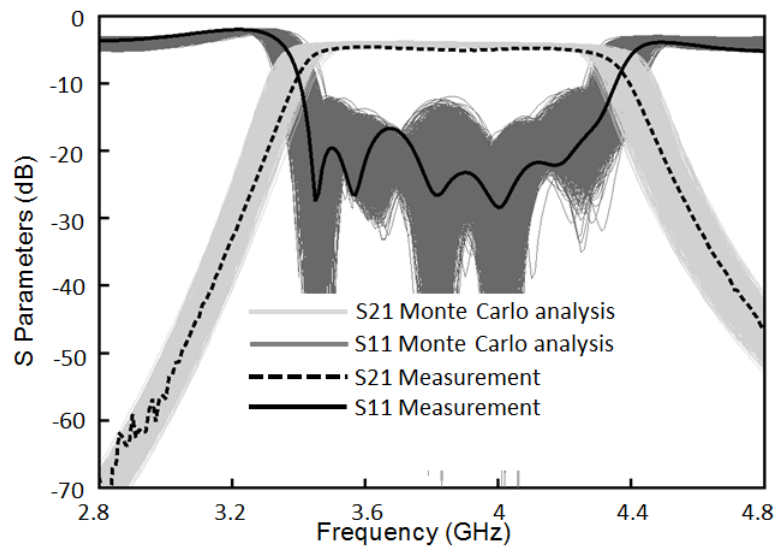


Figure 4.34 – Symmetric absorptive lossy filter: Monte-Carlo analysis considering typical manufacturing tolerances ($8\ \mu\text{m}$ for transmission line dimensions, 1% for relative permittivity, and 2% for engraved resistors). Reprinted with permission from ref. [1]; copyright 2014 IEEE.

The sensitivity analysis performed with the previous tolerances is presented in Figure 4.34. For this design with non-resonating nodes, 59% of realizations met the specifications.

4.5.2. Asymmetric absorptive lossy filters

An asymmetric configuration has been designed applying the same procedure, with attenuation levels set to 6 dB and 1 dB respectively at port 1 and port 2 (Figure 4.36). The network remains identical, but the synthesis leads to another coupling matrix, as shown in Figure 4.35. The layout is presented in Figure 4.37 and the simulated response in Figure 4.38.

	S	1	2	3	4	5	6	7	8	L
S	0	0.3940	0	0	0	0	0	0	0	0
1	0.3940	j0.0113	-0.3974	j0.0167	0	0	0	0	0	0
2	0	-0.3974	j0.0523	0.8543	0	0	0	0	0	0
3	0	j0.0167	0.8543	j0.0792	0.6093	j0.0111	0	0	0	0
4	0	0	0	0.6093	j0.0647	0.5728	j0.0128	0	0	0
5	0	0	0	j0.0111	0.5728	j0.0634	0.5917	0	0	0
6	0	0	0	0	j0.0128	0.5917	j0.1171	0.7908	j0.0517	0
7	0	0	0	0	0	0	0.7908	j0.0527	-0.3660	0
8	0	0	0	0	0	0	j0.0517	-0.3660	j0.0430	0.3875
L	0	0	0	0	0	0	0	0	0.3875	0

Figure 4.35 - Coupling matrix of the asymmetric absorptive lossy network.

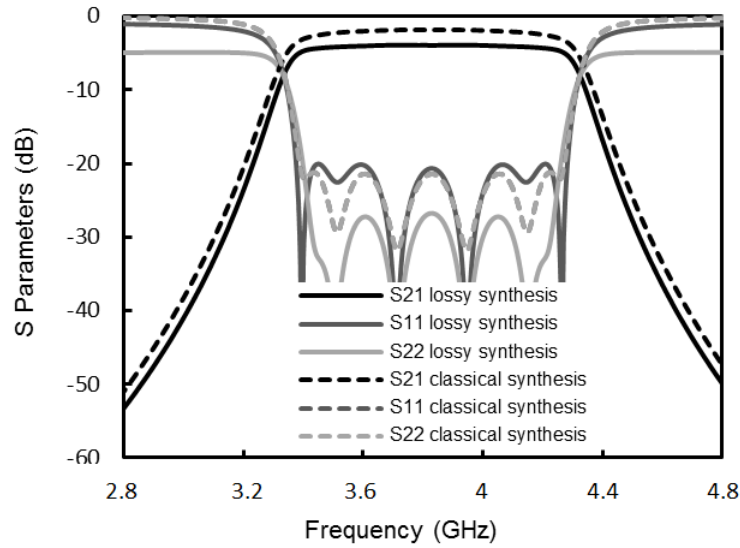


Figure 4.36 - Synthesized response of the asymmetric absorptive lossy network. Reprinted with permission from ref. [1]; copyright 2014 IEEE.

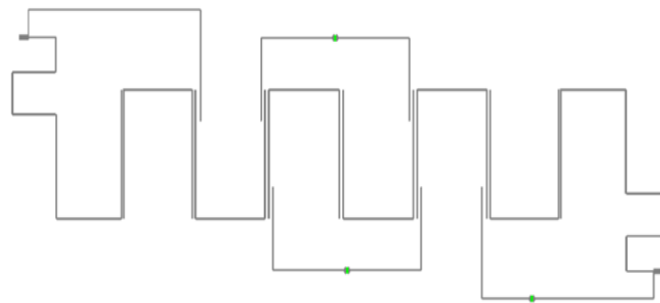


Figure 4.37 - Layout of the asymmetric absorptive lossy filter. Reprinted with permission from ref. [1]; copyright 2014 IEEE.

The insertion loss and the flatness are 4 dB and 0.6 dB respectively. The reflection parameter is 18 dB in the stopband but presents a rebound around 3.3 GHz. As shown in Figure 4.39, measurements agree well with simulations except a slight reduction in the bandwidth and a degradation of the flatness (+0.3 dB). The sensitivity analysis presented in Figure 4.40, shows that 62% of the realizations met the specifications.

Finally, the out-of-band performance (shown in Figure 4.41) is satisfying for both symmetric and asymmetric absorptive lossy filters, considering specifications given in Table 4.1.

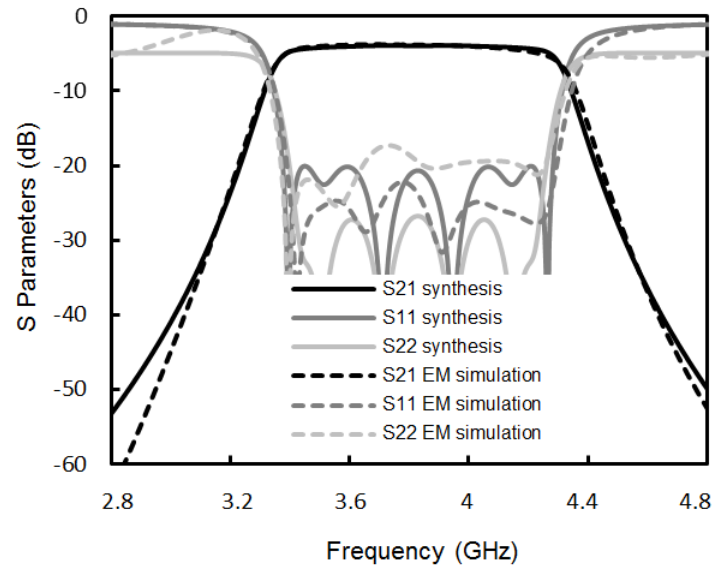


Figure 4.38 - Simulated response of the asymmetric absorptive lossy filter. Reprinted with permission from ref. [1]; copyright 2014 IEEE.

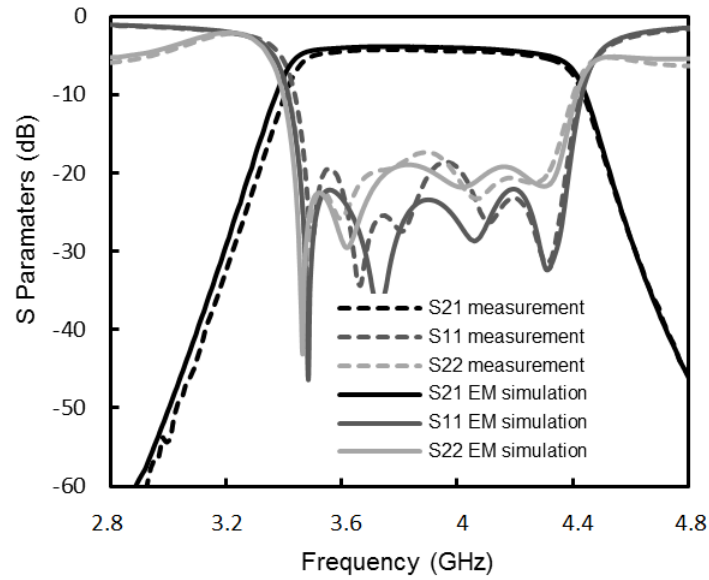


Figure 4.39 - Measured response of the asymmetric absorptive lossy filter. Reprinted with permission from ref. [1]; copyright 2014 IEEE.

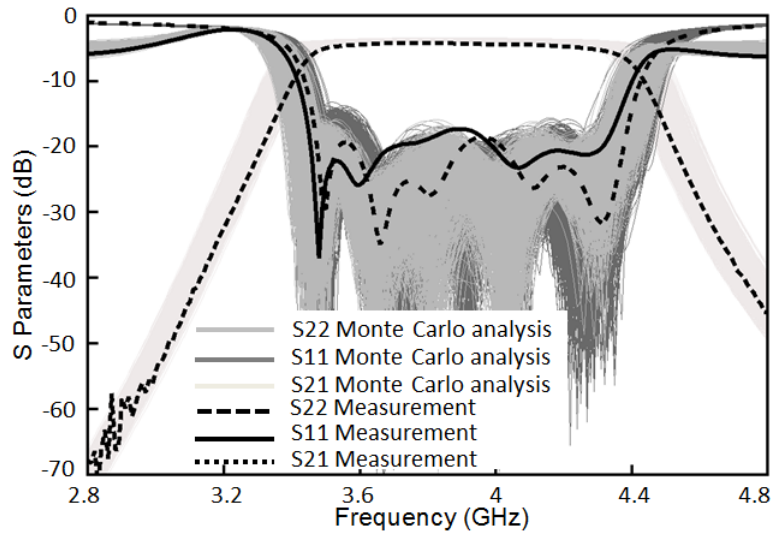


Figure 4.40 – Asymmetric absorptive lossy filter: Monte-Carlo analysis considering typical manufacturing tolerances (8 μm for transmission line dimensions, 1% for relative permittivity, and 2% for engraved resistors). Reprinted with permission from ref. [1]; copyright 2014 IEEE.

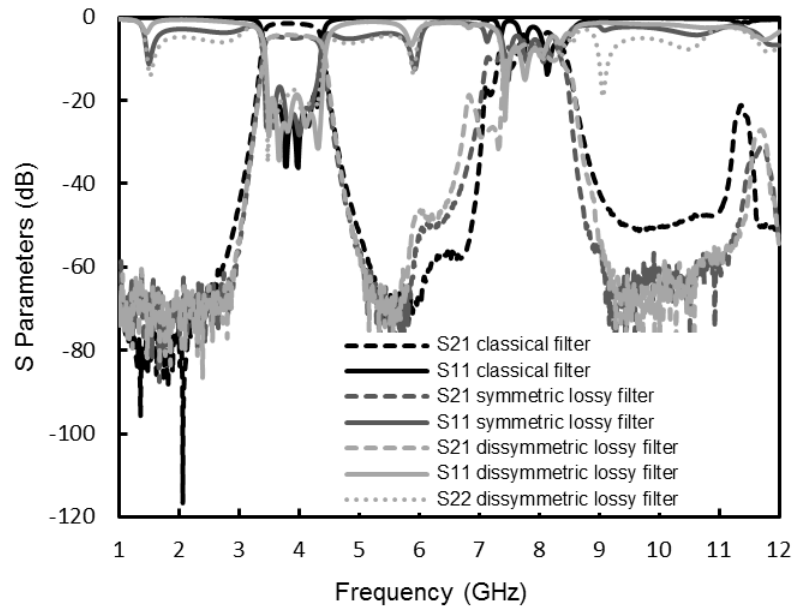


Figure 4.41 - Absorptive lossy filters: measured out-of-band performances. Reprinted with permission from ref. [1]; copyright 2014 IEEE.

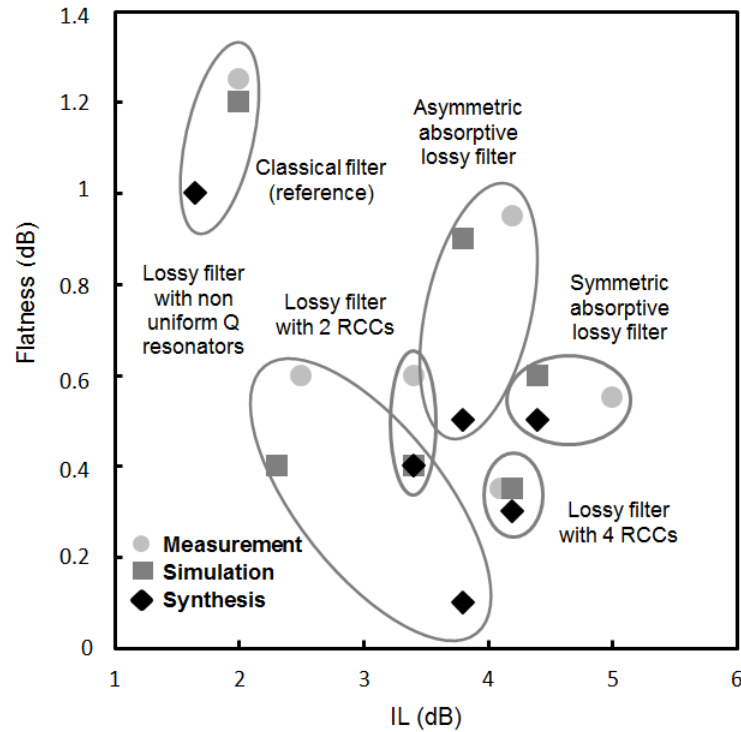


Figure 4.42 - Flatness versus IL for all filters designed in this work. Reprinted with permission from ref. [1]; copyright 2014 IEEE.

Table 4.2 - Measured performances for all filters designed in this work. Reprinted with permission from ref. [1]; copyright 2014 IEEE.

	IL (dB)	Flatness (dB)	RL (dB)	20-dB rejection bandwidth (GHz)	Surface bandwidth (mm ²)
Reference filter	1.9	1.2	20	2.5	210
Transversal lossy filter with non-uniform Q resonators	2.5	0.5	18	0.5	480
In-line lossy filter with 2 RCCs	3.4	0.45	20	2.5	290
In-line lossy filter with 4 RCCs	4.2	0.35	20	2.5	300
Symmetric absorptive lossy filter (4 RCCs and 2 NRNs)	5	0.55	19	2.5	610
Asymmetric absorptive lossy filter (4 RCCs and 2 NRNs)	4.2	0.9	19	2.5	610

4.6. Summary

Several designs of lossy filters for receivers in satellite transponders have been investigated in order to improve the performance in terms of flatness compared to a classical hairpin filter design. Flatness and insertion loss performances for all solutions are summarized in Figure 4.42.

The reference design is a microstrip filter made of coupled hairpin resonators. Two approaches have investigated for improving the flatness of the reference design. Lossy filter designs have been compared to the reference, considering the same specifications and the same technology. An in-line network with resistive cross-couplings and a transversal network with heterogeneous Q resonators

have been designed and fabricated first. Theoretically, the transversal network leads to better performances in terms of flatness, but its implementation is generally difficult, especially considering the input/output junctions between multiple paths, which are naturally dispersive, causing spurious transmissions in the stopband. Moreover, a Monte Carlo analysis has been performed, showing higher sensitivity of this later solution with respect to manufacturing tolerances. Consequently, considering measured performances reported in Table 4.2, in-line networks with resistive cross-couplings appear to be the best solution for implementing our receiver filter. In particular, the version with 2 RCCs appears as a good compromise between flatness and insertion loss. Finally, the in-line network has been transformed introducing non-resonant nodes and additional resistive cross-couplings in order to design absorptive lossy filters. The resulting filters allow attenuating the reflected wave substantially with a reduced impact on the absolute level of losses.

References

- [1] A. Basti, A. Perigaud, S. Bila, S. Verdeyme, L. Estagerie and H. Leblond "Design of microstrip lossy filters for receivers in satellite transponders," *IEEE Trans. Microw. Theory Techn.*, vol. 62, no. 9, pp 2014-2024, Sept. 2014.
- [2] A. Basti, S. Bila, S. Verdeyme, A. Perigaud, L. Estagerie and H. Leblond "Comparison of two approaches for the design of microstrip lossy filters," in *Proc. of 33rd Eur. Microw. Conf. (EuMC)*, Nuremberg, Oct. 2013, pp 21-24.
- [3] M. Meng and I. C. Hunter, "The design of parallel connected filter networks with non-uniform Q resonators," in *2012 IEEE MTT-S Int. Microw. Symp. Dig.*, Montreal (QC), Jun. 2012, pp. 1 -3.
- [4] V. Miraftab and M. Yu, "Advanced coupling matrix and admittance function synthesis techniques for dissipative microwave filters," *IEEE Trans. Microw. Theory Techn.*, vol. 57, no. 10, pp. 2429 -2438, Oct. 2009.
- [5] V. Miraftab and M. Yu, "Generalized lossy microwave filter coupling matrix synthesis and design using mixed technologies," *IEEE Trans. Microw. Theory Techn.*, vol. 56, no. 12, pp. 3016 -3027, Dec. 2008.
- [6] L. Szydlowski, A. Lamecki, and M. Mrozowski, "Design of microwave lossy filter based on substrate integrated waveguide (SIW)," *IEEE Microw. Wireless Compon. Lett.*, vol. 21, no. 5, pp. 249 -251, May 2011.
- [7] I.C. Hunter, V. Dassonville, J.D. Rhodes, "Dual mode filters with conductor loaded dielectric resonators," in *1999 IEEE MTT-S Int. Micro Symp. Dig.*, vol. 3, pp. 1021-1024.
- [8] K. Konno, "Small size combline microstrip narrow BPF", *IEEE Microwave Theory and Techniques Symposium*, Albuquerque, NM, USA, juin 1992.
- [9] I. C. Hunter, R. Ranson, A.C. Guyette, and A. Abunjaileh, "Microwave filter design from a systems perspective", *IEEE Microwave Magazine*, October 2007.
- [10] G. Matthaei, L. Young, and E. M. T. Jones, *Microwave filters, impedance-matching networks, and coupling structures*. Norwood, MA: Artech House, 1980, p. 152
- [11] A.E. Williams, W.G. Bush, R.R. Bonetti, "Predistortion techniques for multicoupled resonator filters", *IEEE Trans. on Micr. Theory and Tech*, 33 (5), 1985.
- [12] S. Bila, P. Lenoir, D. Baillargeat, S. Verdeyme, "Multiple solutions for the synthesis of microwave filters with predistorted transfer functions", *Int. Journal of RF and Micr. Computer-Aided Eng.*, 17 (1), 2007.
- [13] S. Darlington, "Synthesis of a reactance-four pole with prescribed insertion loss characteristics," *J. Math. Phys.*, vol. 18, no 1939, pp. 257-353.
- [14] M. Yu, W-C Tang, A. Malarky, V. Dokas, R. Cameron, Y. Wang, "Predistortion technique for cross-coupled filters and its application to satellite communication systems", *IEEE Trans. on Micr. Theory and Tech*, 51 (12), 2003.
- [15] B. S. Senior, I. C. Hunter, and J. D. Rhodes, "Synthesis of lossy filters," in *Proc. of 32nd Eur. Microw. Conf.*, 2002., pp. 1 -4.
- [16] A. Guyette, I. Hunter, and R. Pollard, "The design of microwave bandpass filters using resonators with nonuniform Q," *IEEE Trans. on Micr. Theory and Tech*, vol. 54, no. 11, pp. 3914-3922, Nov. 2006.
- [17] J. Mateu, A. Padilla, C. Collado, M. Martinez-Mendoza, E. Rocas, C. Ernst, and J. M. O'Callaghan, "Synthesis of 4th order lossy filters with uniform Q distribution," in *2010 IEEE MTT-S Int. Microw. Symp. Dig.*, Anaheim (CA), May 2010, p. 568-571
- [18] L. Szydlowski, A. Lamecki, and M. Mrozowski, "Synthesis of coupled-lossy resonator filters," *IEEE Microw. Wireless Compon. Lett.*, vol. 20, no. 7, pp. 366 -368, Jul. 2010.
- [19] R. J. Cameron, "General coupling matrix synthesis methods for Chebyshev filtering functions," *IEEE Trans. Microw. Theory Techn.*, vol. 47, no. 4, pp. 433 -442, April 1999.
- [20] S. Bila, D. Baillargeat, M. Aubourg, S. Verdeyme, F. Seyfert, L. Baratchart, C. Boichon, F. Thevenon, J. Puech, C. Zanchi, L. Lapierre, and J. Sombrin, "Finite element modelling for the design optimization of microwave filters," *IEEE Trans. Magn.*, Vol 40, no. 2, pp 1472-1475, March 2004
- [21] A. Padilla, J. Mateu, C. Collado, C. Ernst, J. M. Rius, J. M. Tamayo, and J. M. O'Callaghan, "Comparison of lossy filters and

predistorted filters using novel software," in *2010 IEEE MTT-S Int. Microw. Symp. Dig.*, Anaheim (CA), May 2010, p. 1720-1723.

[22] <http://www.tsc.upc.edu/lossyfilters>.

[23] M. Yu and V. MirafTAB, "Shrinking microwave filters," *IEEE Microw. Mag.*, vol. 9, no. 5, pp. 40-54, 2008.